PHYSICAL REVIEW A **76**, 051602(R) (2007)

First- and second-sound-like modes at finite temperature in trapped Fermi gases from BCS to BEC

Yan He, Qijin Chen, Chih-Chun Chien, and K. Levin
James Franck Institute and Department of Physics, University of Chicago, Chicago, Illinois 60637, USA
(Received 14 April 2007; published 8 November 2007)

We determine the temperature (T) dependence of first- and second-sound-like mode frequencies for trapped Fermi gases undergoing the BCS to Bose–Einstein condensation (BEC) crossover. Our results are based on numerical solution of the two-fluid equations in conjunction with a microscopic calculation of thermodynamical variables. As in experiment and at unitarity, we show that the lowest radial breathing mode is T independent. At finite T, higher-order breathing modes strongly mix with second sound. Their complex T dependence should provide an alternative way of measuring the transition temperature T_c.

DOI: 10.1103/PhysRevA.76.051602 PACS number(s): 03.75.Hh, 74.20.Fg, 03.75.Ss, 74.20.De

The recent discovery of the superfluid phases of trapped Fermi gases has led to considerable interest in their collective mode spectrum [1–7]. Among the modes of experimental interest are breathing modes as well as propagating first sound. While originally theoretical attention [8–10] was focused on ground-state properties, experimental measurements are naturally not restricted to temperature $T=0$. Indeed, there is an interesting body of information that is emerging in these Fermi gases about the finite-temperature behavior [4–6] of the breathing modes and, more recently, about the propagating sound velocity [7].

The purpose of this paper is to compute sound mode frequencies in spherically trapped Fermi gases undergoing the BCS to Bose-Einstein condensation (BEC) crossover, at general T. We present a solution of the linearized two-fluid equations and compare with recent experiments. We focus on the radial breathing modes and present predictions for a second-sound-like mode as well. The structure of the two-fluid equations for Bose [11] and Fermi gases [12] has been rather extensively discussed. In the crossover regime, the normal fluid is novel [13,14], containing both fermions and noncondensed pairs, which have not been systematically included in previous collective mode literature.

Of great importance to the field as a whole is the future possibility of second-sound observations, possibly through experiments such as those in Ref. [15]. While existing experimental techniques such as vortex observation [16] and density profile features [17] help establish superfluidity, they provide lower bounds on T_c or determine its value for the special case of a population-imbalanced system. Thermodynamical experiments measure T_c more directly [18,19] but have been confined to unitarity. Thus other techniques, such as second-sound observation, will be of great value. One of the principal results of the present paper is an analysis of how a second-sound-like mode is coupled to the breathing modes. We demonstrate that higher-order breathing modes will reveal T_c through this coupling, and therefore are an alternative to direct second-sound measurements. However, the lowest breathing mode appears to be remarkably T independent at unitarity. This has been observed experimentally [4,5] and argued to follow from isentropic considerations [6]. Here we show that, even when we treat the full coupling between first and second sound, we obtain similar T-independent behavior at unitarity.

At the core of the two-fluid theory is the assumption that hydrodynamics is valid and that there are frequent collisions which produce a state of local thermodynamical equilibrium. Although there are some exceptions [15], reaching the two-fluid regime has not been easy for atomic Bose gases. Two-fluid dynamics are more readily achieved for Fermi gases, principally because in the crossover regime the large scattering lengths produce sufficient collisions. Nevertheless, there has been considerable theoretical interest in setting up [12] and solving [20] the two-fluid equations for Bose condensates. Indeed, hydrodynamical approaches have successfully addressed both the $T=0$ and normal-state regimes of the Bose gases [21]. Here, by contrast, we address the Fermi gas case in a trap. Because they interact more strongly near unitarity, hydrodynamical descriptions have been argued quite convincingly [6,9,22] to be valid.

Previous theoretical work has been confined to $T=0$ treatments of a harmonic trap [8,9] or to finite-T theories [22] of a uniform gas in which there is a clear meaning to "first" and "second" sound. We extend this terminology to a trap, by carefully defining the fingerprints of these modes. Our work is most similar in spirit to an earlier Bose gas study [20], although we introduce different numerical techniques as well as addressing fermions rather than bosons. We note that the input thermodynamics of systems undergoing the BCS-BEC crossover which is used in the present paper has been rather well calibrated against experimental measurements in Ref. [18] and is based on a finite temperature extension of the simplest (BCS-Leggett) ground state. In the absence of a trap our results are for the most part similar to those in Ref. [22].

We begin with the two-fluid equations which describe the dynamical coupling of the superfluid velocity $\mathbf{v}_s$ and the normal velocity $\mathbf{v}_n$. Just as in the spirit of the original Landau two-fluid equations, we ignore viscosity terms. In the presence of a trap potential $V_{\rm ext}=\frac{1}{2}m\omega_{\rm ho}r^2$, the two-fluid equations are given by $m\partial\mathbf{v}_s/\partial t+\boldsymbol{\nabla}(\mu+V_{\rm ext}+m\mathbf{v}_s^2/2)=0$, $\partial\mathbf{j}/\partial t+\boldsymbol{\nabla}\cdot\boldsymbol{\Pi}=-n\boldsymbol{\nabla}V_{\rm ext}$, $\partial n/\partial t+\boldsymbol{\nabla}\cdot\mathbf{j}=0$, and $\partial(ns)/\partial t+\boldsymbol{\nabla}\cdot(ns\mathbf{v}_n)=0$, with $\Pi^{ij}=p\delta^{ij}+n_s\mathbf{v}_s^i\mathbf{v}_s^j+n_n\mathbf{v}_n^i\mathbf{v}_n^j$, $n=n_s+n_n$, and $\mathbf{j}=n_s\mathbf{v}_s+n_n\mathbf{v}_n$. Here μ is the chemical potential, p the pressure, and s the entropy *per particle*. Moreover, we have $n_n\mathbf{v}_n+n_s\mathbf{v}_s=n\mathbf{v}$. Here n_s (v_s) and n_n (v_n) denote the superfluid and normal densities (velocities), respectively. We use the subscript 0 to denote equilibrium quantities such that $\mathbf{v}_{s0}$

$=\mathbf{v}_{n0}=0$, $\nabla(\mu+V_{\text{ext}})=\mathbf{0}$, $\nabla p_0=-n_0\nabla V_{\text{ext}}$, and n_0, s_0, μ_0, and p_0 are independent of time t. Combining this with the thermodynamic relation $d\mu=-sdT+dp/n$, we have $\nabla T_0=0$, implying that the temperature T_0 is constant in the trap. It then follows that in equilibrium $\mu=\mu_0-V_{\text{ext}}$, consistent with the Thomas-Fermi approximation.

For small deviations from equilibrium, we may linearize the two-fluid equations. Eliminating the velocities $\mathbf{v}_s$ and $\mathbf{v}_n$, one finds [12,20]

$$m\frac{\partial^2\delta n}{\partial t^2}=\nabla\cdot\left(n_0\nabla\frac{\delta p}{n_0}\right)-\nabla\cdot(\delta T n_0\nabla s_0), \tag{1}$$

$$m\frac{\partial^2\delta s}{\partial t^2}=\frac{1}{n_0}\nabla\left(\frac{n_{s0}n_0s_0^2}{n_{n0}}\nabla\delta T\right)-(\nabla s_0)^2\delta T+\nabla s_0\cdot\nabla\left(\frac{\delta p}{n_0}\right). \tag{2}$$

We will focus on $\delta\mu(r)$ and $\delta T(r)$ as the principal variables. This choice, which is different from that in Ref. [20], is made because both variables are nonvanishing at the trap edge so that in a basis set expansion they will satisfy the same boundary conditions. Moreover, the two-fluid equations are simplest in this form. Expressing δs, δp, and δn in terms of $\delta\mu$ and δT, the two-fluid equations can be rewritten as

$$\left(\frac{\partial n}{\partial\mu}\right)_T\frac{\partial^2\delta\mu}{\partial t^2}+\left(\frac{\partial n}{\partial T}\right)_\mu\frac{\partial^2\delta T}{\partial t^2}=\frac{A}{m}, \tag{3}$$

$$\left(\frac{\partial s}{\partial\mu}\right)_T\frac{\partial^2\delta\mu}{\partial t^2}+\left(\frac{\partial s}{\partial T}\right)_\mu\frac{\partial^2\delta T}{\partial t^2}=\frac{B}{m}, \tag{4}$$

with

$$A=\nabla\cdot(n\nabla\delta\mu)+\nabla\cdot(ns\nabla\delta T),$$

$$B=\frac{1}{n}\nabla\cdot\left(\frac{nn_s}{n_n}s^2\nabla\delta T\right)+\nabla s\cdot\nabla\delta\mu+s\nabla s\cdot\nabla\delta T.$$

It is understood that all coefficients of $\delta\mu$ and δT are calculated in equilibrium so that we drop the subscript 0. The thermodynamical quantities in equilibrium can be calculated following Ref. [23], based on the standard local density approximation, $\mu(r)=\mu_0-V_{\text{ext}}(r)$. Their derivatives with respect to T and μ can be calculated analytically, and their gradients can be obtained via $\nabla f=-(\partial f/\partial\mu)_T\nabla V_{\text{ext}}$, where f denotes any of the variables (n,n_s,n_n,s).

To solve the two coupled differential equations (3) and (4), we assume a simple harmonic time dependence $\delta\mu,\delta T\propto e^{-i\omega t}$. We cast the differential two-fluid equations into an eigenfunction problem with ω^2 playing the role of eigenvalue and the eigenfunctions given by the amplitudes of $\delta\mu$ and δT. Since neither T nor μ depends on the density, they will not vanish at the trap edge. Our boundary conditions require that all thermodynamic variables be smooth (but not necessarily zero) at the trap edge. At finite T, the density in the trap decreases exponentially when the local chemical potential becomes negative at large radius. We choose, thus, to expand $\delta\mu$ and δT in terms of Jacobi polynomials. For our numerics we choose the matrix dimension to be 300; we have similarly investigated matrices of dimension 200 up to 900, and found little change in our principal findings.

We now turn to an important aspect of our numerics. Because we generate some 300 frequencies in our numerical approach, it is essential to establish a mechanism for systematically identifying first- and second-sound modes. To help find such a "fingerprint," we introduce a "decoupling approximation" based on reducing Eqs. (3) and (4) to $\ddot{\delta\mu}=g_1(\delta\mu,\delta T)$, $\ddot{\delta T}=g_2(\delta\mu,\delta T)$, where $g_{1,2}$ are known functions. We eliminate cross terms by setting $\delta T=0$ in g_1 and $\delta\mu=0$ in g_2. With these two decoupled equations, it is then relatively straightforward to associate a profile plot of the numerically calculated local pressure and entropy vs r within a trap with first- or second-sound-like modes. This procedure can be validated as a zeroth-order approximation to solving the full coupled equations in large part because the breathing mode so obtained is quantitatively very accurate and the sound mode is semiquantitatively consistent. The qualitative T-dependent behavior we find for the first- and second-sound-like modes is not so different from that found elsewhere [20] for Bose gases. An important check on our procedure is that we find that there is no sign of second sound above T_c.

Up to this point everything is general, applying to both Fermi and Bose superfluids. All that is needed is a microscopic theory for thermodynamical variables. Here we use a calculational framework we have developed for treating BCS-BEC crossover in trapped Fermi gases [23–25], which emphasizes the importance of pseudogap effects or finite-momentum pairs. The local thermodynamical potential (density) $\Omega=\Omega_f+\Omega_b$ is associated with a contribution from gapped fermionic excitations Ω_f as well as from noncondensed pairs, called Ω_b. We have

$$\Omega_f=-\frac{\Delta^2}{g}+\sum_{\mathbf{k}}[(\xi_{\mathbf{k}}-E_{\mathbf{k}})-2T\ln(1+e^{-E_{\mathbf{k}}/T})],$$

$$\Omega_b=-Z\Delta^2\mu_{\text{pair}}+\sum_{\mathbf{q}}T\ln(1-e^{-\Omega_{\mathbf{q}}/T}). \tag{5}$$

Here μ_{pair} is the chemical potential of the pairs, which is zero below T_c, and the pair dispersion $\Omega_{\mathbf{q}}$, along with the (inverse) residue Z, can be derived from a microscopic T-matrix theory, described elsewhere [13,14]. Using Ω one then arrives at thermodynamical properties such as the entropy density $ns=-\partial\Omega/\partial T$, as well as self-consistent equations for the total excitation gap Δ, the contribution to Δ from noncondensed pairs (called the pseudogap), and the number equations. These self-consistent (local) equations are simply given by $\partial\Omega/\partial\Delta=0$, $\partial\Omega/\partial\mu_{\text{pair}}=0$, and $n=-\partial\Omega/\partial\mu$, subject to the total number constraint $N=\int d^3r\,n(r)$. When $T<T_c$, we can use the gap equation and chain rule to eliminate the variable Δ, which is a function of μ and T, via $\partial\Delta/\partial\mu=-(\partial^2\Omega_f/\partial\Delta\,\partial\mu)/(\partial^2\Omega_f/\partial\Delta^2)$ and $(\partial\Delta/\partial T)=-(\partial^2\Omega_f/\partial\Delta\,\partial T)/(\partial^2\Omega_f/\partial\Delta^2)$. Similarly, when $T>T_c$ we use the gap and pseudogap equations to eliminate the variables Δ and μ_{pair} to arrive at thermodynamical quantities.

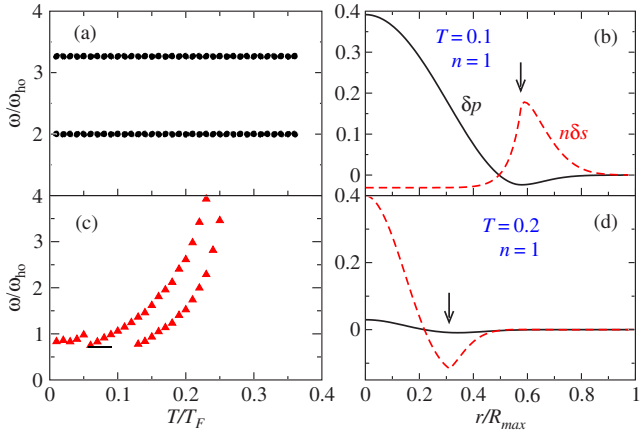

FIG. 1. (Color online) Behavior of the first- (upper row) and second-sound (lower row) modes for a spherical trap at unitarity within the decoupling approximation (see text). The left column shows the T dependence of the frequencies, while the right shows corresponding typical spatial oscillation profiles for δp [(black) solid lines] and $n\delta s$ [(red) dashed lines] at the lowest frequencies, which provide fingerprints of first and second sound. For the second sound, $n\delta s$ dominates and changes sign within the condensate. Here $T_c \approx 0.27 T_F$, and the arrows indicate the condensate edge.

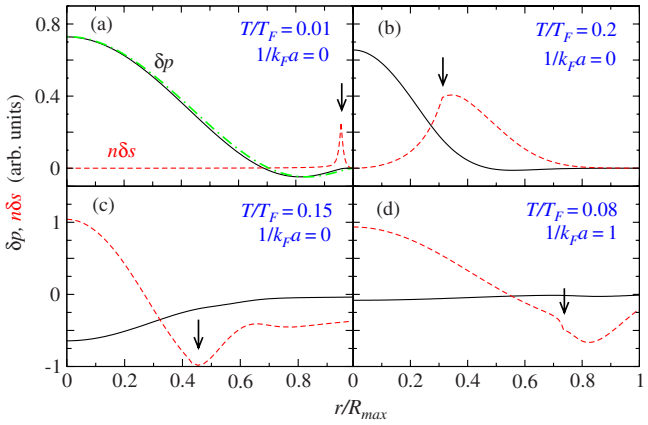

FIG. 2. (Color online) Typical spatial oscillation profiles for δp [(black) solid lines] and $n\delta s$ [(red) dashed lines] obtained from the fully coupled equations for a spherical trap at (a)–(c) unitarity and (d) $1/k_Fa=1$ at different T, for the first- (top row) and second- (bottom row) sound modes. Also shown in (a) is the $T=0$ analytical result [(green) dot-dashed curve]. The arrows indicate condensate edge.

Figure 1 shows the lowest two collective modes at unitarity in a spherical trap, obtained by solving the chemical potential or temperature fluctuation equation in the decoupling approximation scheme described earlier. It is evident that our approximated breathing mode frequency [Fig. 1(a)] is independent of temperature. We understand this result by noting that the decoupled equation for the breathing mode is given by $-\omega^2\delta\mu = C_{\mu\mu 1}\nabla^2\delta\mu + C_{\mu\mu 2}\cdot\nabla\delta\mu$ where $C_{\mu\mu 1} = n(\partial\mu/\partial n)_s$ and $C_{\mu\mu 2} = \nabla\mu$. At unitarity, $n(\partial\mu/\partial n)_s = \frac{2}{3}\mu$. The only T dependence contained in $\mu_0 \equiv \mu(r=0)$ can be eliminated via a simple rescaling of $r \to r\sqrt{2\mu_0/m\omega_{ho}^2}$, yielding a T-independent breathing mode frequency. An important validation of our decoupled breathing mode is that it then becomes equivalent to that obtained from the isentropic assumption of Ref. [6].

By contrast, the second-sound-mode frequency we obtain increases rapidly with temperature. Some typical oscillation profiles of $\delta p(r)$ and $n\delta s(r)$ are shown in the right two panels of Fig. 1. Although the "entropy density oscillations" $n\delta s(r)$ fall off at large r, the entropy per particle $\delta s(r)$ oscillations (not shown) increase very rapidly upon entering the normal region. Consequently, temperature fluctuations δT become large at the trap edge.

Our identification of first sound for the decoupled case leads us to associate this mode in a coupled situation with a profile for which at the trap center δp has a large amplitude, while $n\delta s$ is almost zero (with a small peak near the trap edge) as in Fig. 1(b). By contrast, in the trap center the second-sound mode has large entropy fluctuations, while the pressure fluctuations are almost zero [Fig. 1(d)]. These features will serve as fingerprints for distinguishing (lower-order) first- and second-sound modes at finite temperatures.

Figure 2 shows some typical eigenfunction profiles of the lowest modes obtained in the spherical trap upon solution of the *fully coupled* two-fluid equations. The first row corresponds to the breathing mode in the unitary case. The good agreement between the very low-T result for δp and the $T=0$ analytical solution (green dashed line) in Fig. 2(a) helps validate our numerical scheme. Figure 2(b) corresponds to a high-temperature breathing mode. In this regime the pseudogap region outside the superfluid core is relatively large and the peak in $n\delta s(r)$ is accordingly very broad. The lower two panels correspond to second-sound modes for the unitary and BEC cases. By contrast with the breathing modes, here $n\delta s$ has a larger amplitude than δp with an opposite sign. Clearly this is very similar to what we observed in the decoupled-mode analysis of Fig. 1.

Figures 3(a)–3(c) address the fully coupled equations and show the behavior of the lowest breathing (upper branch) and second-sound mode (lower branch) frequencies as a function of temperature in a spherical trap for $1/k_Fa=1$, 0, and −0.5, respectively. For all three values of $1/k_Fa$ we find very little sign of T_c in the lowest breathing mode frequency. In contrast, the second-sound-mode frequencies increase with T and disappear above T_c. Figure 3(d) presents a more complete series of modes for the unitary case. Here the lines serve as guides to the eye for the lowest (nearly horizontal, blue) and higher-order (green) breathing mode, and second-sound (increasing lines, red) frequencies.

At unitarity [Fig. 3(d)] one can identify a sequence of higher-order breathing modes which precisely overlap with analytical calculations for $T=0$. Importantly, only the lowest of these is found to be a constant in temperature; the others are found to mix with second-sound modes, as indicated in the increasing solid and dashed (red) lines in Fig. 3(d). The behavior of the lowest mode helps to justify the isentropic assumption made in Ref. [6]. We understand this by referring back to the decoupled profiles in Figs. 1(b) and 1(c), which are seen to be quite distinct. By contrast the profiles of the

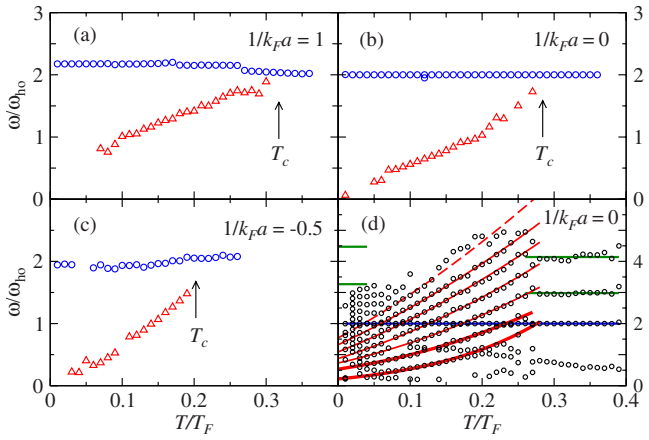

FIG. 3. (Color online) Temperature dependence of breathing mode and second-sound frequencies in a spherical trap. (a)–(c) are for the near-BEC, unitary, and near-BCS cases, respectively. The upper and lower branches in (a)–(c) represent the lowest breathing mode and second-sound frequencies, respectively. In (d), more complete results (open circles) are shown at unitarity, where the lines serve as guides to the eye for the breathing mode (nearly horizontal [blue (lower) and green (upper)] lines) and second sound [increasing (red) curves] frequencies.

decoupled first- and second-sound modes at higher order (notshown) appear more similar to each other than their lowest-order counterparts. Indeed, the behavior of the profiles at higher order is associated with an increasing number of nodes in the curves of δp and $n\delta s$ (not shown), which leads to a greater similarity between first- and second-sound profiles and helps explain why the higher-order modes are more readily mixed [26].

In summary, we have presented predictions for future experiments on higher breathing modes and second sound in a trap. We find that only the lowest breathing mode frequency has very weak T dependence. For the unitary case this temperature insensitivity was clearly observed by Thomas and co-workers [6]. As a result of this experiment it should not be surprising that we find relatively weak dependencies on either side of the Feshbach resonance for this breathing mode frequency. In the literature there are experimental claims (at $1/k_Fa = 1.0$) which are consistent with a decrease [4] in the radial breathing mode frequency, as indeed we find here, although ours is probably too weak to reconcile the different findings in Refs. [4,2,3]. Finally, our more complete studies at unitarity show that, if higher-order radial breathing modes can be accessed, because of their strong hybridization with second sound, it may be possible to use these breathing modes, rather than direct second sound to determine the transition temperatures T_c. This should be of value since there are currently few experiments that can assign a value to T_c over the wider crossover regime.

This work was supported by NSF Grants No. PHY-0555325 and No. MRSEC DMR-0213745. We thank John Thomas for suggesting this problem and Cheng Chin for useful conversations.

[1] C. Chin, M. Bartenstein, A. Altmeyer, S. Riedl, S. Jochim, J. Hecker-Denschlag, and R. Grimm, Science **305**, 1128 (2004).
[2] J. Kinast, S. L. Hemmer, M. E. Gehm, A. Turlapov, and J. E. Thomas, Phys. Rev. Lett. **92**, 150402 (2004).
[3] J. Kinast, A. Turlapov, and J. E. Thomas, Phys. Rev. A **70**, 051401(R) (2004).
[4] A. Altmeyer, S. Riedl, C. Kohstall, M. J. Wright, R. Geursen, M. Bartenstein, C. Chin, J. H. Denschlag, and R. Grimm, Phys. Rev. Lett. **98**, 040401 (2007).
[5] J. Kinast, A. Turlapov, and J. E. Thomas, Phys. Rev. Lett. **94**, 170404 (2005).
[6] J. E. Thomas, J. Kinast, and A. Turlapov, Phys. Rev. Lett. **95**, 120402 (2005).
[7] J. Joseph, B. Clancy, L. Luo, J. Kinast, A. Turlapov, and J. E. Thomas, Phys. Rev. Lett. **98**, 170401 (2007).
[8] H. Hu, A. Minguzzi, X.-J. Liu, and M. P. Tosi, Phys. Rev. Lett. **93**, 190403 (2004).
[9] H. Heiselberg, Phys. Rev. Lett. **93**, 040402 (2004).
[10] G. E. Astrakharchik, R. Combescot, X. Leyronas, and S. Stringari, Phys. Rev. Lett. **95**, 030404 (2005).
[11] A. Griffin and E. Zaremba, Phys. Rev. A **56**, 4839 (1997).
[12] E. Taylor and A. Griffin, Phys. Rev. A **72**, 053630 (2005).
[13] Q. J. Chen, I. Kosztin, B. Jankó, and K. Levin, Phys. Rev. Lett. **81**, 4708 (1998).
[14] Q. J. Chen, J. Stajic, S. N. Tan, and K. Levin, Phys. Rep. **412**, 1 (2005).
[15] D. M. Stamper-Kurn, H.-J. Miesner, S. Inouye, M. R. Andrews, and W. Ketterle, Phys. Rev. Lett. **81**, 500 (1998).
[16] M. W. Zwierlein, J. R. Abo-Shaeer, A. Schirotzek, and W. Ketterle, Nature (London) **435**, 170404 (2005).
[17] M. W. Zwierlein, A. Schirotzek, C. H. Schunck, and W. Ketterle, Science **311**, 492 (2006).
[18] J. Kinast, A. Turlapov, J. E. Thomas, Q. J. Chen, J. Stajic, and K. Levin, Science **307**, 1296 (2005).
[19] L. Luo, B. Clancy, J. Joseph, J. Kinast, and J. E. Thomas, Phys. Rev. Lett. **98**, 080402 (2007).
[20] V. B. Shenoy and T.-L. Ho, Phys. Rev. Lett. **80**, 3895 (1998).
[21] A. Griffin, W.-C. Wu, and S. Stringari, Phys. Rev. Lett. **78**, 1838 (1997).
[22] H. Heiselberg, Phys. Rev. A **73**, 013607 (2006).
[23] Q. J. Chen, J. Stajic, and K. Levin, Phys. Rev. Lett. **95**, 260405 (2005).
[24] J. Stajic, Q. J. Chen, and K. Levin, Phys. Rev. Lett. **94**, 060401 (2005).
[25] Y. He, C.-C. Chien, Q. J. Chen, and K. Levin, arXiv:0707.1751.
[26] There exists a lower-ω first-sound-like mode at $T \neq 0$, which we also find in the "free" (but hydrodynamic) Fermi gas limit.